International Journal of Osteoarchaeology
Int. J. Osteoarchaeol. **21**: 732–742 (2011)
Published online 22 June 2010 in Wiley Online Library
(wileyonlinelibrary.com) DOI: 10.1002/oa.1185

A Case of Valgus Ankle in an Early Pleistocene Hominin

J. M. DESILVA[a]* AND **A. PAPAKYRIKOS**[b]

[a] *Department of Anthropology, Boston University, Boston, MA 02215, USA*
[b] *Cushing Academy, Ashburnham, MA, USA*

ABSTRACT Bipedal locomotion is a defining character of the hominin lineage. A skeletal correlate of bipedality is a perpendicularly oriented tibia relative to the plane of the ankle joint, positioning the foot directly under the centre of mass. Non-human primates, in contrast, possess a tibial shaft that tilts laterally away from the plane of the ankle joint (valgus ankle), which positions the foot in inversion and is adaptive for arboreal climbing. KNM-ER 2596 is a small distal tibia from 1.9 mya sediments at Koobi Fora, Kenya. Though it possesses some morphologies functionally linked to bipedality, such as an expanded metaphysis, it also possesses a valgus tilt to the ankle. We test the competing hypotheses that the KNM-ER 2596 tibia is from a cercopithecoid, a non-human hominoid, or a pathological hominin. A survey of the orthopaedic literature and a comparative study of modern human and non-human primate tibiae support the hypothesis that KNM-ER 2596 is from a hominin. In order to investigate the non-phylogenetic causes of valgus ankle, we examined human skeletal tibiae with valgus tilt secondary to fracture of the distal fibula. Untreated breaks of the lower third portion of the fibula during childhood can result in a valgus tilt to the distal tibia and occasionally other peculiar morphologies found in the KNM-ER 2596 tibia such as a superoinferiorly atrophied medial malleolus. The morphology of this tibia is incompatible with hypotheses that it is from a cercopithecoid or a hominoid, and instead, we suggest that KNM-ER 2596 belonged to a hominin that may have suffered a fracture of the lower left fibula as a juvenile.

Key words: distal tibia; fracture; fibula; paleopathology

Introduction

KNM-ER 2596 is a small distal tibia recovered from Area 15 of the Upper Burgi Member at the productive Kenyan fossil locality, Koobi Fora (Leakey & Walker, 1985; Figure 1). It has been dated to approximately 1.89 ± 0.05 million years (Feibel *et al.*, 1989). This fossil has not been described in detail but was identified by Leakey & Walker (1985) as a hominin. Because of the difficulty in confidently assigning isolated postcranial remains to one of the several hominin taxa coexisting during the early Pleistocene, we refer to the fossil by its accession number and not any particular species throughout this paper. Notes left by two researchers at the National Museum of Kenya, however, suggest that KNM-ER 2596 may be from a *Theropithecus* monkey, and not a hominin. This is the first thorough treatment of this fossil.

* Correspondence to: Boston University, Department of Anthropology, 232 Bay State Road, Boston, MA 02215, USA.
e-mail: jdesilva@bu.edu

The distal tibia has been a particularly useful element to distinguish bipedal hominins from non-human primates (Latimer *et al.*, 1987; DeSilva, 2009). Latimer *et al.* (1987) found humans possess a perpendicularly oriented tibial shaft relative to the horizontal plane of the ankle joint. This morphology, together with the bicondylar angle of the distal femur, positions both the knee and the ankle directly under the centre of mass during bipedal gait. Additionally, this morphology of the human distal tibia orients the foot such that the plantar aspect of the foot faces inferiorly. In contrast, non-human primates possess a tibial shaft that tilts laterally away from the horizontal plane of the ankle joint (Latimer *et al.*, 1987; DeSilva, 2008, 2009). This morphology positions the plantar aspect of the foot in inversion and is a morphology adaptive to the positions of foot inversion utilised by non-human primates during climbing bouts (DeSilva, 2009). For this angular measure, all known hominin distal tibiae (except KNM-ER 2596) from 4.1 million years to present, possess a human-like perpendicularly oriented tibial shaft (Latimer *et al.*, 1987; Ward *et al.*, 1999; DeSilva, 2009).

Received 11 September 2009
Revised 5 May 2010
Accepted 13 May 2010

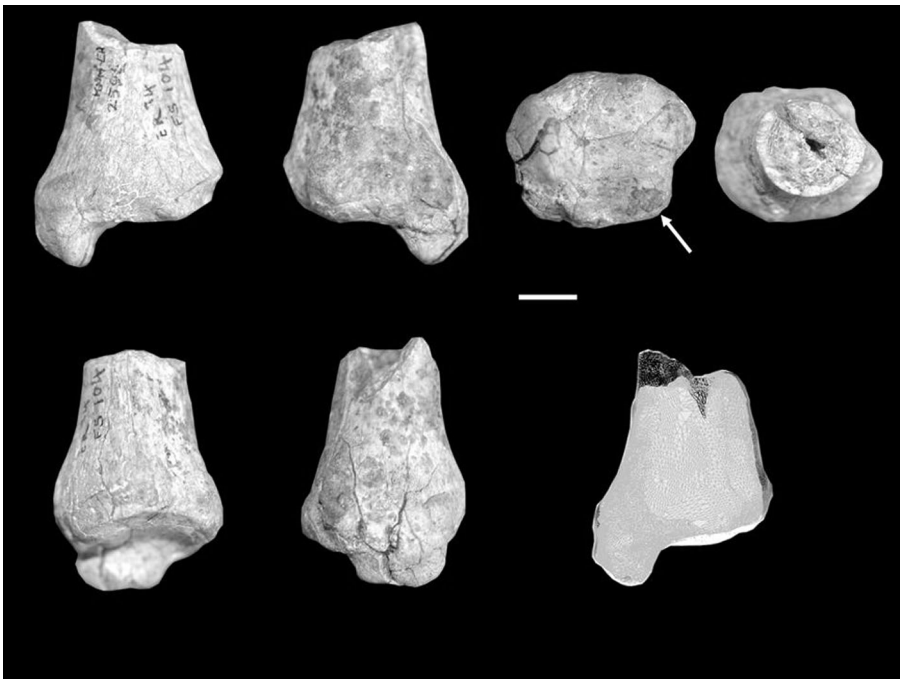

Figure 1. KNM-ER 2596. Top (left to right): anterior, posterior, inferior and superior views. Bottom (left to right): lateral, medial views and a digital coronal cross-section. Notice in the lateral view the human-like expanded metaphysis relative to the width of the tibial shaft. Also notice the valgus tilt to the talar articular surface. The white arrow points to a possible osteophytic growth on the posterolateral aspect of the articular rim. Scale bar = 1 cm.

In addition to the orientation of the plane of the ankle joint, it has been suggested that human tibiae differ from non-human primates in possessing an anteroposteriorly expanded metaphysis (Leakey *et al.*, 1995; Kunos & Latimer, 2000; Ward *et al.*, 2001). This morphology adapts the ankle joint to the high loads incurred during bipedal locomotion. Additionally, it has been found that the talar articular facet of African ape distal tibiae has a mediolaterally expanded anterior aspect, adaptive for loading in positions of extreme dorsiflexion during climbing bouts (DeSilva, 2009). The talar facet of the ape distal tibia thus looks like a trapezoid, whereas humans and all hominins have a square-shaped distal end, adaptive for loading in positions of moderate dorsiflexion and plantarflexion incurred during bipedal walking (DeSilva, 2009).

In this context, we first describe the KNM-ER 2596 tibia and then test the three competing hypotheses that this tibia belongs to: (1) a cercopithecoid, (2) a non-human hominoid and (3) a pathological hominin.

Materials and methods

KNM-ER 2596 was compared to distal tibiae of modern taxa detailed in Table 1 and shown in Figure 2. To assess whether the valgus ankle of the tibia might be the result of trauma to the missing fibula, 43 adult human tibiae from individuals documented to have suffered a fibular fracture during life were studied at the Cleveland Museum of Natural History. KNM-ER 2596 was also compared to fossil distal tibiae of hominins and cercopithecoids from the Plio-Pleistocene (Table 2 and Figure 2). Six measurements were taken on the talar articular surface of the distal tibia: the maximum mediolateral width of the anterior, posterior and

Table 1. Extant distal tibiae studied

Family	Species	Male	Female	Sex unknown	Total
Hominoid	*Homo sapiens*	25	34	18	77
	Pan spp.	21	21	11	53
	Gorilla gorilla gorilla	23	19	2	44
Cercopithecoid	*Papio* spp.	18	7	12	37
	Nasalis larvatus	18	19	0	37

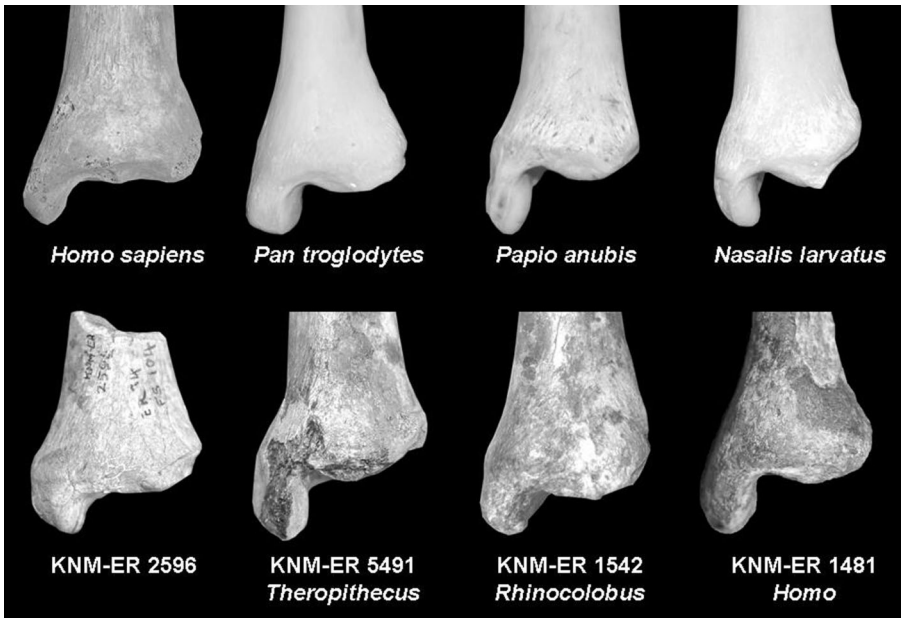

Figure 2. Comparative tibiae examined in this study. KNM-ER 2596 (lower left) was compared to the distal tibia of extant primates representing (top from left to right) humans, African apes (chimpanzee shown here), terrestrial Old World monkeys (baboon shown here), and arboreal Old World monkeys (proboscis monkey shown here). Additionally, KNM-ER 2596 was compared to other early Pleistocene distal tibiae from Koobi Fora, Kenya including those of terrestrial and arboreal monkeys (*Theropithecus* and *Rhinocolobus*, respectively) and fossil hominins. All of the bones in this figure have been scaled to roughly the same size, and KNM-ER 1542 has been reversed to reflect the left side.

midpoint regions of the articular surface, and the maximum anteroposterior length of the most medial, lateral and midpoint aspects of the articular surface. Each raw measure was then normalised by the geometric mean, following a size adjustment protocol (Darroch & Mosimann, 1985). The maximum mediolateral width of the distal tibial metaphysis was measured just superiorly to the medial malleolus but did not include the medial malleolus in the measurement. The anteroposterior dimension of the metaphysis was measured as the maximum distance perpendicular to the mediolateral width. The thickness of the medial malleolus was taken at the midpoint of the malleolus at its most superior junction with the articular surface of the distal tibia, and is reported here as a ratio of the maximum anteroposterior length of the medial malleolus. Metaphyseal expansion was calculated as a ratio of the anteroposterior width of the metaphysis divided by the anteroposterior width of the talar articular surface at its midpoint.

The angle that the long axis of the tibia forms with the distal articular surface of the tibia was measured using a carpenter's contour guide. The tibiae were pressed into the carpenter's contour guide with the contour pins parallel to the long axis of the tibial shaft. The contour guide was then laid flat, and the impression made by the articular surface of the tibia was photographed with a Nikon D100 digital camera. The images were imported into the program Image J and the angle formed between the articular surface and the long axis of the tibia as inferred by the unmoved straight contour pins was measured. This procedure was done on a cast of KNM-ER 2596. In addition, the original fossil tibia was scanned with a Next Engine portable 3D desktop laser scanner at the maximum resolution possible of 0.1 mm. The 3D model was imported into the program ScanStudio, and digitally sectioned in the coronal plane. An image of the digitally sectioned fossil was imported into Image J, where the angle formed between the long axis of the tibia and the articular joint surface was measured with the angle tool as described above. There were no differences between the two methods.

Results

Description of KNM-ER 2596 and comparative morphometrics

KNM-ER 2596 is a distal tibia preserving 41.8 mm from the tip of the medial malleolus to a break in the tibial

Table 2. Fossil tibiae measured in this study

Subfamily	Accession number	Geological age	Probable species	Body mass estimate (kg)[a]
Hominin?	KNM-ER 2596	1.89[b]	Unknown	24.8 (human model)
Hominin	KNM-KP 29285	4.12[c]	*Australopithecus anamensis*	42.9
Hominin	A.L. 333-6	3.2[d]	*A. afarensis*	31.1
Hominin	A.L. 333-7	3.2[d]	*A. afarensis*	43.3 (est.)
Hominin	A.L. 288-1	3.18[d]	*A. afarensis*	24.9
Hominin	StW 181	2.6–2.8[e]	*A. africanus*	32.7 (est.)
Hominin	StW 358	2.6–2.8[e]	*A. africanus*	24.4
Hominin	StW 389	2.6–2.8[e]	*A. africanus*	34.2
Hominin	StW 514b	2.6–2.8[e]	*A. africanus*	28.5 (est.)
Hominin	KNM-ER 1481	1.9[b]	*Homo habilis? H. erectus?*	42.9
Hominin	KNM-ER 1500	1.9[b]	*A. boisei?*	36.7
Hominin	OH 35	1.85	*H. habilis? A. boisei?*	28.7
Hominin	StW 567	1.4–1.7[e]	*Homo*	37.6
Hominin	KNM-WT 15000	1.5[f]	*H. erectus*	58.3
Colobine	KNM-ER 1542	1.87–2.08[g]	*Rhinocolobus turkanaensis*	32.3
Colobine	KNM-ER 45613	1.56–1.87[g]	*R. turkanaensis*	29.9
Cercopithecine	KNM-ER 3823	1.87–2.08[g]	*Theropithecus oswaldi*	21.8
Cercopithecine	KNM-ER 3877	1.87–2.08[g]	*T. oswaldi*	23.4
Cercopithecine	KNM-ER 5474	1.56–1.87[g]	*T. oswaldi*[h]	31.8
Cercopithecine	KNM-ER 40443	1.38–1.87[g]	*T. oswaldi*	38.5
Cercopithecine	KNM-ER 597	1.38–1.56[g]	*T. oswaldi*	27.1
Cercopithecine	KNM-ER 866	1.38–1.56[g]	*T. oswaldi*	57.9
Cercopithecine	KNM-ER 5491	1.38–1.56[g]	*T. oswaldi*	38.5
Cercopithecine	KNM-WT 16755	1.4–2.1[i]	*T. oswaldi*	15.0
Cercopithecine	KNM-WT 16875	1.4–2.1[i]	*T. oswaldi*	29.4
Cercopithecine	KNM-OG 1109	>0.74[i]	*T. oswaldi*	27.6

[a] Hominin estimates based on average of three human-regression equations from McHenry (1992). Body mass estimates of cercopithecoids based on Equations provided in Rafferty *et al*. (1995).
[b] Feibel *et al*. (1989).
[c] Leakey *et al*. (1998).
[d] Walter (1994).
[e] Kuman & Clarke (2000), Pickering *et al*. (2004).
[f] Walker & Leakey (1993).
[g] Jablonski & Leakey (2008).
[h] Papionini gen. et sp. Indet. in Jablonski & Leakey (2008).
[i] Krentz (1993).

shaft (Figure 1). The superior break is fairly uniform and horizontal to the long axis of the tibial shaft except posteromedially, where a triangular fragment of bone is missing. The shaft dimensions at the break are 19.6 mm mediolateral and 17.5 mm anteroposterior. Cortical bone is exposed at the point of the break and is thickest laterally (3.2 mm), with the other dimensions: anterior 2.0 mm, posterior 2.9 mm and medial 2.9 mm. KNM-ER 2596 is 31.7 mm at its widest mediolaterally and 25.9 mm at its widest anteroposteriorly. These dimensions correspond to the location of the metaphysis, and demonstrate the greatly expanded metaphyseal region. Relative to the anteroposterior length of the articular surface, modern humans and fossil hominins possess a greatly expanded metaphysis. In contrast, cercopithecoids and hominoids possess a greatly reduced metaphyseal volume. For this measure, KNM-ER 2596 is in the human range, and well outside the range of any non-human anthropoid (Figure 3). The fossil is relatively well preserved, though there are numerous cracks along all aspects of the bone. These suggest that the bone remained on the surface for some time before deposition and is best categorised as taphonomic stage 1 (Behrensmeyer, 1978). There is a small squatting facet 7.6 mm mediolaterally and 4.6 mm superoinferiorly. Along the posterior surface, an eroded though detectable malleolar groove for the posterior tibialis tendon runs inferomedially. A very faint epiphyseal line runs along the rim of the distal tibia and can be detected in certain areas of the bone, especially anterolaterally. Because this epiphyseal line is almost obliterated, the individual represented by KNM-ER 2596 was near-adult.

Laterally, there is a complete absence of a fibular facet, unlike the condition found in modern apes. The anterior tibiofibular crest is low in relief and moderately thick. It terminates in a small tubercle, which is 4.3 mm

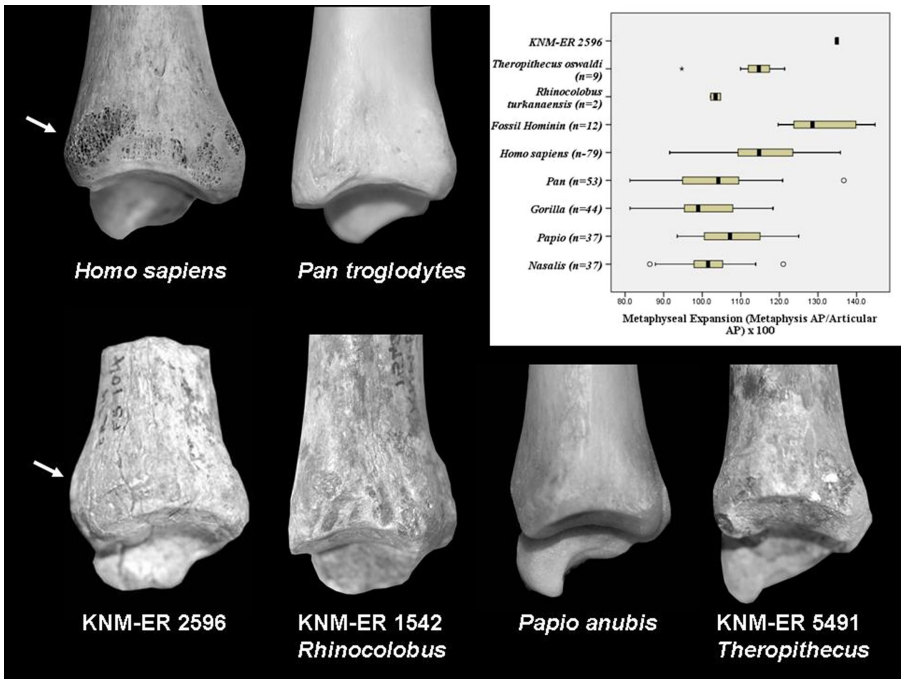

Figure 3. In lateral view, the expanded metaphysis can be seen on the human distal tibia (arrow). Non-human primates, in contrast, do not have an expanded metaphyseal volume of the distal tibia. As indicated by the graphed results, KNM-ER 2596 is quite human-like for this important bipedal feature, falling outside the range for all non-human primates, suggesting strongly that this fossil tibia belongs to a hominin. All of the bones in this figure have been scaled to roughly the same size, and KNM-ER 1542 has been reversed to reflect the left side. For this and all subsequent figures, the median (black bar), interquartile range (box) and overall ranges (whiskers) are illustrated. Outliers defined as 1.5 times the interquartile range are shown as circles.

superior to the talar articular surface. The posterior tibiofibular crest is much weaker in its development, producing only a faint rugosity on the lateral surface of the fossil. The crest terminates inferiorly in an enlarged posterior tibiofibular tuberosity that extends towards the posterior aspect of the bone. In lateral view, the posterior rim of the talar articular surface projects slightly more inferiorly than the anterior rim, a feature typical of most hominin distal tibiae. In this view, it can also be seen that the articular surface is extremely flat, and does not possess the concave shape and depth found in hominins and cercopithecoids. Posteroinferiorly, there is a small, inferiorly projecting feature, possibly a small osteophytic growth (indicated with an arrow in Figure 1).

The medial malleolus is atrophied superoinferiorly, projecting only 5.7 mm from the talar articular surface. The malleolus itself is relatively thin, only 8.9 mm in mediolateral thickness and 15.9 mm in its anteroposterior dimension, both taken at the junction of the malleolus and the talar articular surface. Non-human hominoids have a mediolaterally thick medial malleolus (Figure 4), a bony adaptation for loading the ankle joint in positions of inversion (DeSilva, 2008). In contrast, KNM-ER 2596 resembles cercopithecoids and hominins. However, superiorly, where the medial malleolus joins the tibial metaphysis, the malleolus bulges medially. The lateral surface of the medial malleolus is flat, quite unlike the bulbous morphology found in cercopithecoids. Medially, there are several cracks running superoinferiorly through the malleolus, the thickest of which is 1.26 mm and results in a slight exaggeration of both the anteroposterior and mediolateral dimensions of the medial malleolus. Overall, however, the cracks do not appear to have dramatically changed the dimensions of this structure. Medially, there are also several small circular punctures in the bones that may represent tooth impressions. The inferiorly and posteriorly positioned attachment on the medial malleolus for the posterior tibiotalar portion of the deltoid ligament is weakly developed. This morphology is quite unlike that found in cercopithecoids and hominins, and instead resembles the weak attachment for the posterior tibiotalar ligament. found in non-human hominoids. The malleolus is angled anteromedially, a condition found in many hominoids, though it does not greatly expand the anterior aspect of the articular surface as found in the African apes.

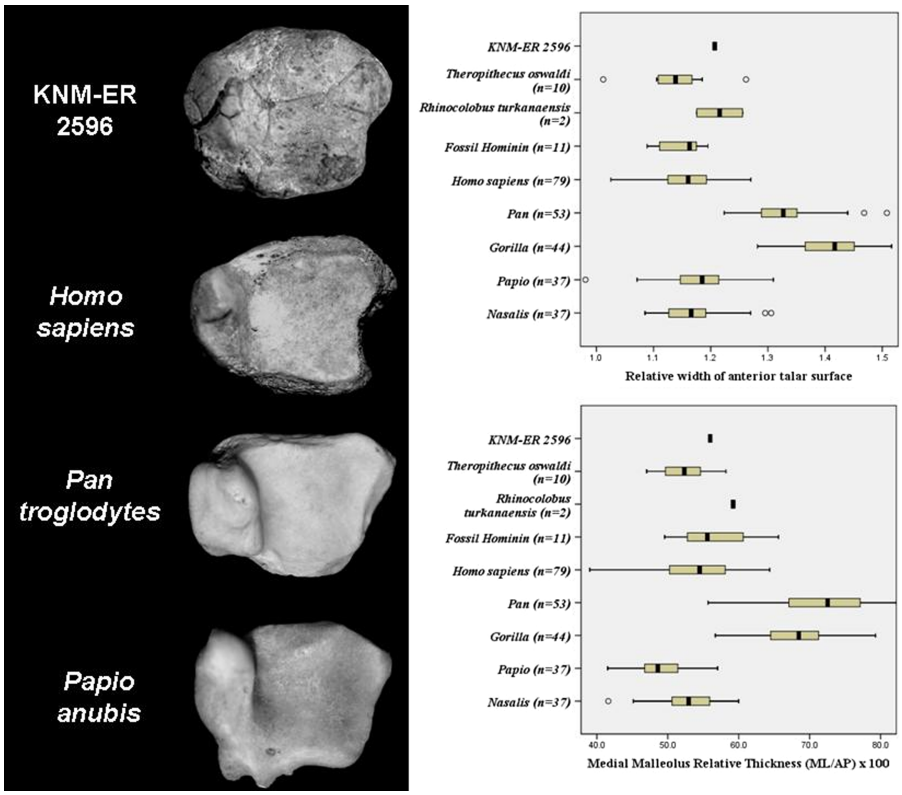

Figure 4. In inferior view, two important morphologies of the African ape ankle are clear. First, apes have a mediolaterally broad anterior aspect of the talar articular surface (top graph). This feature results in a trapezoid-shaped talar articular surface in contrast to the square-shaped surface found in humans and monkeys. Second, apes have a mediolaterally thick medial malleolus (bottom graph). Both morphologies are related to ape-like vertical climbing (see text for details). For both of these morphologies, KNM-ER 2596 is quite unlike the tibiae of chimpanzees and gorillas, and instead resembles humans and monkeys. All of the bones in this figure have been scaled to roughly the same size.

The talar articular surface is relatively flat, and does not possess the strong median keel typical of cercopithecoid and most hominoid tibiae. There is a faint, though palpable keel that divides the talar articular surface in the unequal midpoint dimensions of approximately 10 mm medially and 8.0 mm laterally. The entire talar surface itself is slightly wedged, with the mediolateral dimensions: 21.5 mm anteriorly, 18.0 mm at midpoint and 14.4 mm posteriorly. Non-human hominoids possess a mediolaterally wide anterior aspect of the talar articular surface, an adaptation for loading during positions of extreme dorsiflexion (Figure 4, DeSilva, 2009). For this feature, KNM-ER 2596 is decidedly unlike African apes, and instead falls within the distribution of hominins and cercopithecoids. The anteroposterior dimensions of the talar articular surface are: 18.6 mm laterally, 18.9 mm at midpoint and 16.3 mm medially. The talar articular surface is obliquely oriented relative to the long axis of the tibial shaft, a so-called valgus ankle. An angle of $\sim 103^{\circ}$ is estimated, with a range of 99–107°, due to the fragmentary nature of the fossil. The valgus orientation of the talar surface of KNM-ER 2596 can be well accommodated within the range of variation found in the non-human primates measured in this study, but falls well outside the range of both modern and fossil hominins (Figure 5). There are several small circular punctures in the talar articular surface, including one located along the junction of the articular surface and the medial malleolus from which several cracks radiate. These small circular punctures could be the result of carnivore activity.

Based on the talar articular dimensions of the tibia, this bone belonged to an individual roughly 25 kg if using a human regression model (McHenry, 1992), and 28 kg if using a hominoid model (RMA in McHenry, 1992). A catarrhine model for calculating body mass (Rafferty *et al.*, 1995) yields an estimate of 33 kg. Estimated body size alone does not preclude KNM-ER 2596 from belonging to an extinct hominin, non-human hominoid, or cercopithecoid (Table 2).

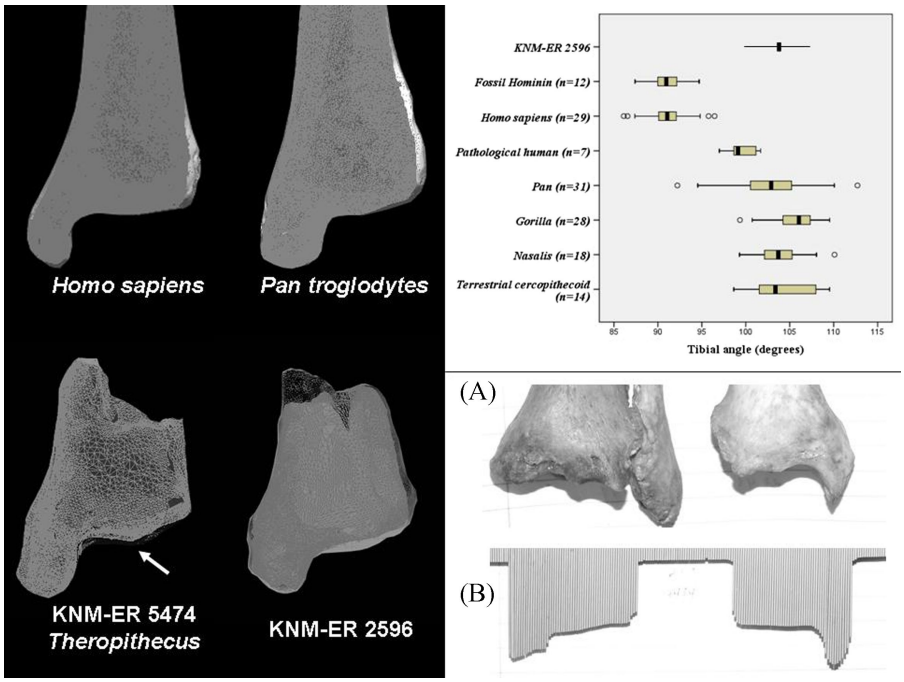

Figure 5. Unlike humans and extinct hominins, KNM-ER 2596 possesses a valgus tilt to the talar articular surface. Additionally, in contrast to the talar articular surface of cercopithecoids which have a strong central keel (arrow pointing to keel of KNM-ER 5474), the surface of KNM-ER 2596 is relatively flat. These morphologies are best explained as a by-product of an unhealed fibular fracture (see text for details). (A) A healed fibula fracture (left) is shown relative to the ipsilateral tibia (right). (B) The resulting valgus angles measured using a carpenter's contour tool are shown. Notice that the left tibia has a valgus tilt, while the right tibia illustrates the typical human perpendicular set to the ankle joint. The range of values for the valgus set to the KNM-ER 2596 tibia falls within the range measured in modern humans with a pathological valgus ankle condition. The cross-sections in this figure have been scaled to roughly the same size.

Pathological analysis

Forty-three adult human skeletons with a healed fibula fracture were examined at the Cleveland Museum of Natural History (Hamann–Todd collection). All of these skeletons were from adults and the fibula break had healed and produced a detectable callus. Eighteen of these fibula breaks were associated with tibia breaks on the ipsilateral leg. For these individuals, a valgus ankle was not present. There were 18 individuals who possessed only a fibula break, but did not have a valgus angle to the distal tibia. Eleven of these individuals had broken either the middle portion, or the proximal portion of the fibula, while seven individuals had broken the distal fibula. Of the 43 skeletons studied, seven possessed a valgus ankle oriented on average $8.1 \pm 2.4^{\circ}$ more laterally than the contralateral leg (Table 3). The average valgus angle of these individuals was $99.6 \pm 1.7^{\circ}$ (range: 97.0–101.7°), a value near though still below the estimated valgus ankle of KNM-ER 2596 (Figure 5). For all of these individuals, the location of the fibula break was limited to the distal third of the fibula. Thus, 50% of those individuals with a break of the distal third of the fibula, but not a tibial fracture, possessed a valgus orientation to the distal tibia. For those individuals that had a normal morphology to the distal tibia, we suggest that they may have fractured their fibula as adults, and thus the break did not impact the angular orientation of the unfused distal tibial epiphysis.

Similar to KNM-ER 2596, several of the individuals with fibula breaks and valgus tibiae also had superoinferiorly atrophied medial malleoli. Of the seven individuals with valgus angles to the distal tibia, two had negligible (<5%) differences in the superoinferior height of the malleolus. The other five exhibit substantially atrophied medial malleoli of: 10%, 16%, 20%, 57% and 77% of the medial malleolar heights of the contralateral tibia. Flattening of the joint surface did not appear to be a common feature and, in fact, several tibiae were found in which the depth was clearly increased by the development of osteophytes along the anterior and posterior rims. Nevertheless, at least one specimen possessed a flattened tibial joint surface relative to the contralateral tibia. Thus, all of the unusual morphologies of the KNM-ER 2596 can be found to varying degrees in tibiae of individuals with a fracture of the distal third of the fibula.

Table 3. Valgus ankle measurements in human specimens with a healed fibular fracture

Specimen number	Tibial angle of leg with ipsilateral fibula break	Tibial angle of contralateral leg	Difference
HTH 1677	100.9°	93.4°	7.5°
HTH 1973	101.4°	90.4°	11.0°
HTH 887	98.5°	89.2°	9.3°
HTH 1448	98.8°	93.6° (healed break)	5.2°
HTH 1381	101.7°	92.3°	9.4°
HTH 1434	97.0°	92.3°	4.7°
HTH 219	99.1°	89.2°	9.9°
Average	99.6 ± 1.7°	91.5 ± 1.9°	8.1 ± 2.4°

Discussion

KNM-ER 2596 possesses a mixture of morphologies not present in any non-pathological extant anthropoid (Table 4). Distal tibiae of humans and extinct hominins are characterised by a perpendicularly oriented tibia over the foot and a deeply concave articular surface of the distal tibia which would limit inversion and dorsiflexion, respectively (DeSilva, 2008). However, for both of these measures, the distal tibia KNM-ER 2596 is unlike modern or fossil humans. The fossil tibia has an obliquely orientated shaft over the articular surface, and a shallow depth of the articular surface. However, even though these morphologies suggest that this individual would have been able to achieve positions of inversion and dorsiflexion at the ankle, there is little evidence that the ankle was frequently loaded in these joint positions. The medial malleolus does not have the relative thickness found in modern ape medial malleoli, and also unlike apes, this tibia does not possess the broad anterior surface adaptive for bouts of vertical climbing. There is also the complete absence of a distal fibular facet, which implies that unlike apes, this individual did not have a strong grasping hallux. These morphologies render the hypothesis that KNM-ER 2596 belonged to a non-human ape untenable.

The obliquely tilted tibia, square-shaped articular facet, thin medial malleolus, and absence of a distal fibular facet are all features present to varying degrees in cercopithecoid distal tibiae. However, this bone is not from the similarly sized Pleistocene monkey *Theropithecus oswaldi*. The distal tibiae of *Theropithecus* have very strongly keeled anteroposteriorly directed midlines, and the medial malleolus has both a bulbous anteromedial portion and a deep intercollicular groove for the posterior tibiotalar ligament. In contrast, KNM-ER 2596 has a mediolaterally flat tibial surface, and a very weak attachment for the posterior tibiotalar ligament on an anteromedially flat medial malleolus.

However, there is another large-bodied primate from the Upper Burgi Member of the Koobi Fora deposits, the colobine *Rhinocolobus turkanaensis* (Leakey, 1982). There are two distal tibiae identified as coming from *Rhinocolobus*: KNM-ER 1542 and KNM-ER 45613. *Rhinocolobus* tibiae, like KNM-ER 2596, have a relatively flat anteromedial portion of the medial malleolus, and a more mediolaterally flattened articular surface of the distal tibia when compared to *Theropithecus*. KNM-ER 2596, however, possesses a key morphology thought to be related to bipedality: an expanded metaphysis.

The metaphysis of KNM-ER 2596 is expanded to a degree only found in modern humans and hominins (Figure 3). This expanded metaphyseal volume has been argued to be an adaptation for absorbing the large forces incurred during bipedalism (Kunos & Latimer, 2000) and has been used as evidence for bipedality in

Table 4. Mixture of traits possessed by KNM-ER 2596

	Cercopithecoid	Hominoid	Hominin
Tibial angle	Yes	Yes	No
Tibial articular surface dimensions	Yes	No	Yes
Medial malleolus thickness	Yes	No	Yes
Medial malleolus morphology	No	Yes	Yes
Depth of tibial articular surface	No	Yes	No
Metaphyseal expansion	No	No	Yes
Lack of fibular facet	Yes	No	Yes (though variable)
Flat tibiotalar surface	No	No (though variable)	Yes (though variable)

early hominins (Leakey *et al.*, 1995; Ward *et al.*, 2001). Importantly, *Rhinocolobus* does not have this expanded volume. In fact, the presumably more terrestrial *Theropithecus* possesses a larger relative metaphyseal volume than *Rhinocolobus*, though still significantly less than what is present in KNM-ER 2596. The hypothesis that KNM-ER 2596 was misidentified as a hominin and instead is a distal tibia from the large-bodied cercopithecoid *Rhinocolobus* is therefore problematic for the following reasons. First, support for this hypothesis would require a substantial increase in the variation known for *Rhinocolobus*, and may suggest a significant degree of terrestriality in this colobine. Second, support for this hypothesis would imply that an expanded metaphyseal volume is not solely a bipedal adaptation and thus its utility in identifying hominins in the fossil record would be limited. Though these two scenarios are possible, we find it more likely that KNM-ER 2596 is a hominin, but one with a valgus deformity of the ankle.

Valgus ankle

In an assessment of a modern human osteological collection, we found that half ($n = 7$ out of 14) of the individuals with a fracture of the distal fibula, but not the distal tibia, develop a valgus ankle. In addition, these tibiae often possess an atrophied medial malleolus, a morphology found on the KNM-ER 2596 tibia.

Orthopaedic studies have found that several types of trauma can cause a valgus ankle deformity in young humans, including a fracture to the proximal or distal tibia, malunion of a fractured fibula, and syndesmosis injuries (Wiltse, 1972; Bluman & Chiodo, 2008). Many of these ankle injuries result in a lateral shift in pressure within the ankle mortise, in some cases causing loss of cartilage, and increased joint stress (Bluman & Chiodo, 2008). The tibiotalar tilt itself is formed when increased stress on the lateral side of the tibia slows the growth of the lateral physis (Hsu *et al.*, 1974; Dias, 1978; Griffiths & Wandtke, 1981; Burkus *et al.*, 1983).

This stress can be caused by any condition that decreases tibiotalar contact area. Fibular shortening and rotation, damage to the deltoid ligament, and/or a lateral shift of the talus within the ankle joint were found to increase peak pressures in the ankle, by decreasing tibiotalar contact (Ramsey & Hamilton, 1976; Curtis *et al.*, 1992). In many of these situations, especially those involving trauma, deltoid ligament damage can occur (Bluman & Chiodo, 2008). This fact is important to note due to the weak attachment area for the posterior tibiotalar portion of the deltoid ligament on KNM-ER 2596.

Fibular shortening has been observed in cases of paralysis, growth plate abnormalities and trauma (Wiltse, 1972; Hollingsworth 1975; Karrholm *et al.*, 1984). In children with neuromuscular disorders, reduced muscle activity in the lower limb impedes normal maturation of the fibular epiphysis, causing a shortening of the bone (Makin, 1965). In addition to a valgus ankle, fibular shortening can also result in a shallow and unstable ankle joint (Makin, 1965; Dias, 1978), a noteworthy morphology given the shallow joint present in KNM-ER 2596. Cases of ankle trauma in which growth arrest of the distal fibula has occurred more than 2 years prior to skeletal maturity lead to the development of fibular shortening, and the resulting valgus tilt to the ankle joint (Karrholm *et al.*, 1984). Interestingly, however, these same characteristics were described by Hollingsworth (1975) in children with spina bifida and by Makin (1965) in children with poliomyelitis and valgus flatfoot. However, patients with valgus ankle as a result of spina bifida or poliomyelitis have a prominent medial malleolus (Hsu *et al.*, 1974; Hollingsworth, 1975), unlike the atrophied medial malleolus found in KNM-ER 2596.

Yet another cause of valgus ankle is posterior tibial tendon deficiency (PTTD), one of the several causes of adult flat foot deformity (Gibson & Prieskorn, 2007). PTTD is associated with hypertension, diabetes, obesity and trauma (Holmes & Mann, 1992). The elongation of the posterior tibial tendon in the initial stages of PTTD allows the calcaneus and other bones of the foot to rotate laterally, producing a heel valgus (Johnson & Strom, 1989). The valgus tilt of the heel causes a lateral displacement of the Achilles tendon relative to the subtalar joint and initiates the shortening of the gastrocnemius–soleus complex (Myerson, 1996; Meehan & Brage, 2003). As the disorder proceeds the deltoid ligament weakens, resulting in a valgus tilt of the tibiotalar joint (Myerson, 1996; Gibson & Prieskorn, 2007; Bluman & Chiodo, 2008). Possible consequences of PTTD include degeneration of the lateral tibial plafond and stress fractures of the fibula (Norris & Mankin, 1978; Myerson, 1996; Bluman & Chiodo, 2008).

There are many other pathologies responsible for valgus ankle that produces osseous deformities that are not assessable in KNM-ER 2596 due to its fragmentary nature. These deformations include tibial bowing in congenital absence of the fibula (Coventry & Johnson, 1952) and exaggerated tibial torsion in neuromuscular disorders (Makin, 1965). In addition, hereditary multiple exostoses (HME), a disorder of the growth

plates, can cause valgus ankle (Solomon, 1961). Although we find a fibula fracture the most likely cause of the valgus tilt in KNM-ER 2596, there are many other causes of valgus ankle in modern humans that should be noted here. These include: cerebral palsy, rheumatoid arthritis, Charcot disease, tarsal coalition, skeletal dysplasias, hemophilia, neurofibromatosis, osteochondromas (bone tumors) and Ollier's disease (Dias, 1978; Griffiths & Wandtke, 1981; Keenan *et al.*, 1991; Skyrme *et al.*, 2003; Bluman & Chiodo, 2008; Wani *et al.*, 2009).

Using a system developed by Bluman & Chiodo (2008) for categorizing valgus ankle, KNM-ER 2596 best matches the morphological description of type I or II valgus deformity. Type I deformity was found by Bluman & Chiodo (2008) primarily in tibial pilon fractures, and malunion of a distal tibial and fibular fractures. They described Type II deformity in cerebral palsy, pseudoarthrosis of the fibula, poliomyelitis and myelomeningocele (Bluman & Chiodo, 2008), conditions either unlikely to have afflicted an early Pleistocene hominin, or at least conditions that would have rendered the hominin unlikely to reach near-adult age. Therefore, we find it most likely that KNM-ER 2596 is the earliest case of a Type I valgus ankle deformity in the human fossil record, caused most likely by an unhealed distal fibular fracture.

Conclusion

The distal tibia KNM-ER 2596 possesses an expanded metaphysis and is thus most likely from a hominin. The presence of a valgus tilt to the talar articular surface can be best explained as the pathological result of an unhealed fracture to the distal third of the ipsilateral fibula. KNM-ER 2596 may therefore be the earliest evidence of a Type I valgus ankle deformity in the fossil record.

Acknowledgements

The authors are grateful to E. Mbua, the National Museums of Kenya, and the Kenyan Ministry of Education, Science and Technology for permission to study the ER 2596 fossil, and for allowing us to study additional fossils in their care. Thanks to B. Zipfel for facilitating access to the Sterkfontein fossils. Hominin casts were studied thanks to Y. Haile-Selassie and D. Pilbeam. We are grateful to the following individuals who provided access to skeletal collections: J. Chupasko, B. Stanley, K. Zyskowski, E. Westwig, L. Gordon, and O. Lovejoy. Particular thanks to L. Jellema for assistance at the Cleveland Museum of Natural History. Thanks the L. MacLatchy and two reviewers for thoughtful comments that improved this paper. This work was made possible thanks to funding by the Leakey Foundation.

References

Behrensmeyer AK. 1978. Taphonomic and ecological information from bone weathering. *Paleobiology* **4**: 150–162.

Bluman EM, Chiodo CP. 2008. Valgus ankle deformity and arthritis. *Foot and Ankle Clinics of North America* **13**: 443–470.

Burkus JK, Moore DW, Raycroft JF. 1983. Valgus deformity of the ankle in myelodysplastic patients. Correction by stapling of the medial part of the distal tibial physis. *The Journal of Bone and Joint Surgery* **65**: 1157–1162.

Coventry MB, Johnson EW. 1952. Congenital absence of the fibula. *The Journal of Bone and Joint Surgery* **34**: 941–955.

Curtis M, Michelson JD, Urquhart MW, Byank RP, Jinnah RH. 1992. Tibiotalar contact and fibular malunion in ankle fractures. A cadaver study. *Acta Orthopaedica* **63**: 326–329.

Darroch JN, Mosimann JE. 1985. Canonical and principle components of shape. *Biometrika* **72**: 241–252.

DeSilva JM. 2008. Vertical climbing adaptations in the anthropoid ankle and midfoot: implications for locomotion in Miocene catarrhines and Plio-Pleistocene hominins. *PhD Dissertation*, University of Michigan.

DeSilva JM. 2009. Functional morphology of the ankle and the likelihood of climbing in early hominins. *Proceedings of the National Academy of Sciences* **106**: 6567–6572.

Dias LS. 1978. Ankle valgus in children with myelomeningocele. *Developmental Medicine and Child Neurology* **20**: 627–633.

Feibel CS, Brown FH, McDougall I. 1989. Stratigraphic context of fossil hominins from the Omo group deposits: Northern Turkana basin, Kenya and Ethiopia. *American Journal of Physical Anthropology* **78**: 595–622.

Gibson V, Prieskorn D. 2007. The valgus ankle. *Foot and Ankle Clinics of North America* **12**: 15–27.

Griffiths H, Wandtke J. 1981. Tibiotalar tilt: a new slant. *Skeletal Radiology* **6**: 193–197.

Hollingsworth RP. 1975. An X-ray study of valgus ankles in spina bifida children with flat foot deformity. *Proceedings of the Royal Society of Medicine* **68**: 481–484.

Holmes GB, Mann RA. 1992. Possible epidemiological factors associated with rupture of the posterior tibial tendon. *Foot and Ankle* **13**: 70–79.

Hsu LCS, O'Brien JP, Yau ACMC, Hodgson AR. 1974. Valgus deformity of the ankle on children with fibular pseudarthrosis: results of the treatment by bone-grafting of the fibula. *Journal of Bone and Joint Surgery (Am)* **56**: 503–510.

Jablonski N, Leakey MG. 2008. *Koobi Fora Research Project*. Vol. 6, The Fossil Monkeys. California Academy of Sciences: San Francisco.

Johnson KA, Strom DE. 1989. Tibialis posterior tendon dysfunction. *Clinical Orthopaedics and Related Research* **239**: 196–206.

Karrholm J, Hansson LI, Selvik G. 1984. Changes in tibiofibular relationships due to growth disturbances after ankle fractures in children. *The Journal of Bone and Joint Surgery* **66**: 1198–1210.

Keenan MA, Peabody TD, Gronley JK, Perry J. 1991. Valgus deformities of the feet and characteristics of gait in patients who have rheumatoid arthritis. *The Journal of Bone and Joint Surgery* **73**: 237–247.

Krentz HB. 1993. Postcranial anatomy of extant and extinct species of *Theropithecus*. In *Theropithecus: The Rise and Fall of a Primate Genus*, Jablonski N, (ed.). Cambridge University Press: Cambridge; 383–424.

Kuman K, Clarke RJ. 2000. Stratigraphy, artifact industries and hominin associations for Sterkfontein, Member 5. *Journal of Human Evolution* **38**: 827–847.

Kunos CA, Latimer B. 2000. Cross-sectional geometric properties of the distal tibial metaphysis in humans and apes. *American Journal of Physical Anthropology (Suppl.)* **30**: 202–203.

Latimer B, Ohman JC, Lovejoy CO. 1987. Talocrural joint in African hominoids: implications for *Australopithecus afarensis*. *American Journal of Physical Anthropology* **74**: 155–175.

Leakey MG. 1982. Extinct large colobines from the Plio-Pleistocene of Africa. *American Journal of Physical Anthropology* **58**: 153–172.

Leakey MG, Feibel CS, McDougall I, Walker A. 1995. New four-million-year-old hominid species from Kanapoi and Allia Bay, Kenya. *Nature* **376**: 565–571.

Leakey MG, Feibel CS, McDougall I, Ward C, Walker A. 1998. New specimens and confirmation of an early age for *Australopithecus anamensis*. *Nature* **393**: 62–66.

Leakey REF, Walker AC. 1985. Further hominids from the Plio-Pleistocene of Koobi Fora, Kenya. *American Journal of Physical Anthropology* **67**: 135–163.

Makin M. 1965. Tibio-fibular relationship in paralyzed limbs. *The Journal of Bone and Joint Surgery (Br)* **47**: 500–506.

McHenry HM. 1992. Body size and proportions in early hominids. *American Journal of Physical Anthropology* **87**: 407–431.

Meehan RE, Brage M. 2003. Adult acquired flat foot deformity: clinical and radiographic examination. *Foot and Ankle Clinics of North America* **8**: 431–452.

Myerson MS. 1996. Adult acquired flatfoot deformity. Treatment of dysfunction of the posterior tibial tendon. *The Journal of Bone and Joint Surgery (Am)* **78**: 780–792.

Norris SH, Mankin HJ. 1978. Chronic tenosynovitis of the posterior tibial tendon with new bone formation. *The Journal of Bone and Joint Surgery (Am)* **60**: 523–526.

Pickering TR, Clarke RJ, Moggi-Cecchi J. 2004. Role of carnivores in the accumulation of the Sterkfontein Member 4 hominid assemblage: a taphonomic reassessment of the complete hominid fossil sample (1936–1999). *American Journal of Physical Anthropology* **125**: 1–15.

Rafferty KL, Walker AC, Ruff CB, Rose MD, Andrews PJ. 1995. Postcranial estimates of body weight in *Proconsul*, with a note on a distal tibia from Napak, Uganda. *American Journal of Physical Anthropology* **97**: 391–402.

Ramsey PL, Hamilton W. 1976. Changes in tibiotalar are of contact caused by lateral talar shift. *The Journal of Bone and Joint Surgery (Am)* **58**: 356–357.

Skyrme AD, Chana R, Selmon GPF, Butler-Manual A. 2003. Osteochondroma of the distal tibia leading to deformity and stress fracture of the fibula. *Foot and Ankle Surgery* **9**: 129.

Solomon L. 1961. Bone growth in diaphysial aclasis. *The Journal of Bone and Joint Surgery* **43**: 700–716.

Walker AC, Leakey RF. 1993. *The Nariokotome Homo erectus Skeleton*. Harvard University Press: Cambridge.

Walter RC. 1994. Age of Lucy and the first family: laser $^{40}Ar/^{39}Ar$ dating of the Denen Dora member of the Hadar Formation. *Geology* **22**: 6–10.

Wani IH, Sharma S, Malik FH, Singh M, Shiekh I, Salaria AQ. 2009. Distal tibial interosseous osteochondroma with impending fracture of fibula: a case report and review of literature. *Cases Journal* **2**: 115.

Ward CV, Leakey MG, Walker A. 2001. Morphology of *Australopithecus anamensis* from Kanapoi and Allia Bay, Kenya. *Journal of Human Evolution* **41**: 255–368.

Ward CV, Leakey MG, Walker AC. 1999. The new hominid species *Australopithecus anamensis*. *Evolutionary Anthropology* **7**: 197–205.

Wiltse LL. 1972. Valgus deformity of the ankle: a sequel to acquired or congenital abnormalities of the fibula. *Journal of Bone and Joint Surgery (Am)* **54**: 595–606.

